Quantitative time-stretch imaging flow cytometry for high-throughput cell-cycle analysis

Aaron T.Y. Mok[1], Kelvin C.M. Lee[1], Kenneth K.Y. Wong[1], and Kevin K. Tsia[1,*]
[1]Department of Electrical and Electronic Engineering, The University of Hong Kong, Pokfulam, Hong Kong
* Email: tsia@hku.hk

We present an image-based cell-cycle analysis at single-cell precision measured by a multimodal time-stretch imaging flow cytometer with a throughput >10,000 cells/sec. Flow cytometry is a potent tool for cellular phenotyping, which hold the keys to understand cellular functions [1]. However, it lacks the ability to detect and quantify biophysical phenotypes of cells, an effective intrinsic marker to probe a multitude of cellular processes. A notable example is cell growth, regarded as "one of the last big unsolved problems in cell biology" [2]. Although quantitative-phase microscopy (QPM) enables cell growth studies by quantifying the cell size and dry mass in a label-free manner, it has largely been restricted to adherent cell analysis with a low imaging throughput of ~100's cells [3,4]. This limitation hampers high-throughput single-cell analysis which is now an unmet need in detection and analysis of rare metastatic cancer cells in a large population (thousands to even millions of cells) [3-6].

Leveraging its ultrafast frame rate, biophysical single-cell imaging based on time-stretch technology has shown its potential in scaling the imaging throughput by at least 2 orders of magnitude higher than the current techniques [7-9]. Here we present a further advancement by developing a multimodal time-stretch imaging flow cytometer for high-throughput image-based cell cycle analysis of cancer cells (metastatic breast cancer cell line, MDA-MB-231). The system features both QPM and fluorescence detection of individual suspended cells, flowing in a polydimethylsiloxane-based microfluidic channel at a high throughput of 10,000 cells/sec. Its configuration is similar to that reported in ref. [8-10] except an additional module for fluorescence excitation and detection. Fig. 1 shows some representative bright-field and quantitative-phase cell images captured by the system.

Not only can the system performs biophysical phenotyping inferred from the QPM, but also quantify the DNA content of single-cells with DNA-specific fluorescence labels. The combined information can be utilized for cell-growth monitoring and characterization of cell-cycle phases. The fluorescence signal is first used to identify the cell-cycle phase of individual cells and revealed the distribution of the cell-cycle phases in the whole population with G1/S/G2M phase, as 57.3%, 18.4% and 24.3% respectively (Inset of Fig. 2). Cell growth is then quantified by the cell dry mass which represents the protein content of each cell [11]. Throughout the cell-cycle, a progressive increase in dry mass from G1 (286±4 pg), via S (357±8 pg) to G2/M (438±11 pg) is observed ($p < 0.01$) (Fig. 2). Furthermore, our analysis combining dry mass and fluorescence signal reveals that faster cell growth occurs in G1 and G2/M phases, in comparison to that during the S phase. It is consistent to the dominating action of DNA content duplication in this phase [12]. In summary, this integrated time-stretch imaging flow cytometer (QPM plus fluorescence detection) presents a powerful tool for large-scale single-cell analysis based on both molecular signatures (e.g. DNA content) and biophysical markers (e.g. dry mass) – opening a new paradigm in single-cell analysis of basic biology and new mechanistic insights into disease processes, not limited to cancer cell growth.

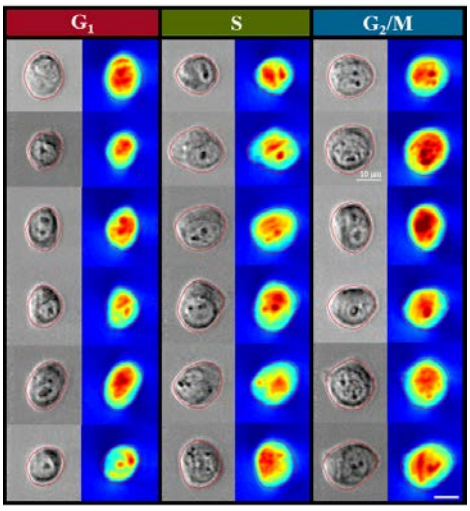

Fig. 1. Bright-field and quantitative phase images of cell in different cell cycle phase are shown with scale bar representing 10 µm. Red contour indicating the cell boundary.

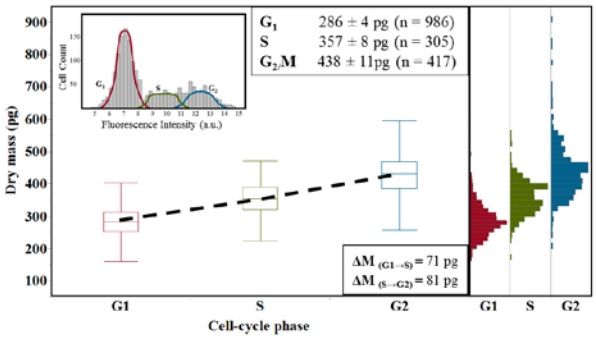

Fig 2. Dry mass in different cell-cycle phases. Dry mass increases from phase G1 at 286 ± 4 pg (α = 0.01, n = 986) to phase S at 357 ± 8 pg (α = 0.01, n = 305), and finally G2/M phase at 438 ± 11 pg (α = 0.01, n = 417). (Inset) Distribution of the fluorescence intensities based on 1,708 cells.

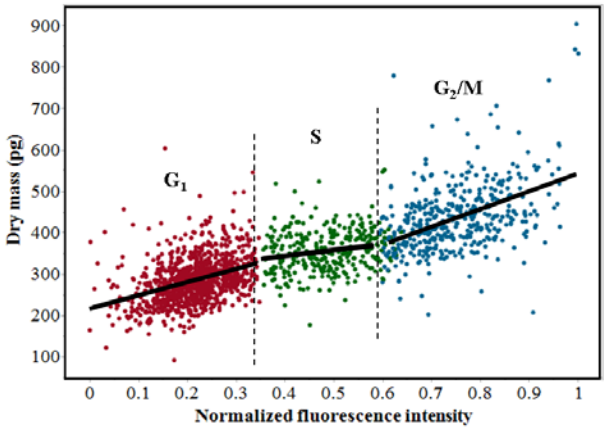

Fig 3. Dry mass versus normalized fluorescence intensity on the same data set shown in Fig. 2 (n = 1,708).

REFERENCES:

[1] M. Brown, and C. Wittwer, Clin Chem 46, 1221-1229 (2000).
[2] J. B. Weitzman, Journal of Biology 2, 3 (2003).
[3] M. Mir, Z. Wang, Z. Shen, M. Bednarz, R. Bashir, I. Golding, S. G. Prasanth, and G. Popescu, Proc Natl Acad Sci USA 108, 13124-13129
[4] P. Girshovitz, and N. T. Shaked, Biomed Opt Express 3, 1757-1773 (2012).
[5] H. Murad, M. Hawat, A. Ekhtiar, A. AlJapawe, A. Abbas, H. Darwish, O. Sbenati, and A. Ghannam, Cancer Cell Int 16, 39 (2016).
[6] J. Y. Hong, H. J. Chung, S. Y. Bae, T. N. Trung, K. Bae, and S. K. Lee, J Cancer Prev 19, 273-278 (2014).
[7] K. Goda, A. Ayazi, D. R. Gossett, J. Sadasivam, C. K. Lonappan, E. Sollier, A. M. Fard, S. C. Hur, J. Adam, C. Murray, C. Wang, N. Brackbill, D. Di Carlo, and B. Jalali, Proc Natl Acad Sci U S A 109, 11630-11635 (2012).
[8] T. T. Wong, A. K. Lau, K. K. Ho, M. Y. Tang, J. D. Robles, X. Wei, A. C. Chan, A. H. Tang, E. Y. Lam, K. K. Wong, G. C. Chan, H. C. Shum, and K. K. Tsia, Sci Rep 4, 3656 (2014).
[9] A. K. Lau, T. T. Wong, K. K. Ho, M. T. Tang, A. C. Chan, X. Wei, E. Y. Lam, H. C. Shum, K. K. Wong, and K. K. Tsia, J Biomed Opt 19, 76001 (2014).
[10] C. L. Chen, A. Mahjoubfar, L. C. Tai, I. K. Blaby, A. Huang, K. R. Niazi, and B. Jalali, Sci Rep 6, 21471 (2016).
[11] R. Barer, Nature 169, 366-367 (1952).
[12] K.A. Schafer, Vet. Pathol 35, 461-478 (1998).